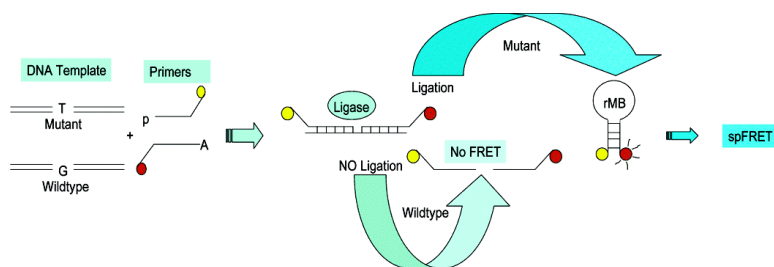


## Approaching Real-Time Molecular Diagnostics: Single-Pair Fluorescence Resonance Energy Transfer (spFRET) Detection for the Analysis of Low Abundant Point Mutations in K-ras Oncogenes

Musundi B. Wabuyele, Hannah Farquar, Wieslaw Stryjewski, Robert P. Hammer, Steven A. Soper, Yu-Wei Cheng, and Francis Barany

*J. Am. Chem. Soc.*, **2003**, 125 (23), 6937-6945 • DOI: 10.1021/ja034716g • Publication Date (Web): 17 May 2003

Downloaded from <http://pubs.acs.org> on March 29, 2009



### More About This Article

Additional resources and features associated with this article are available within the HTML version:

- Supporting Information
- Links to the 11 articles that cite this article, as of the time of this article download
- Access to high resolution figures
- Links to articles and content related to this article
- Copyright permission to reproduce figures and/or text from this article

[View the Full Text HTML](#)



## Approaching Real-Time Molecular Diagnostics: Single-Pair Fluorescence Resonance Energy Transfer (spFRET) Detection for the Analysis of Low Abundant Point Mutations in K-ras Oncogenes

Musundi B. Wabuyeleye,<sup>†</sup> Hannah Farquar,<sup>†</sup> Wieslaw Stryjewski,<sup>†</sup> Robert P. Hammer,<sup>†</sup> Steven A. Soper,<sup>\*,†</sup> Yu-Wei Cheng,<sup>‡</sup> and Francis Barany<sup>‡</sup>

*Contribution from the Department of Chemistry, Louisiana State University, Baton Rouge, Louisiana 70803 and Department of Microbiology, Joan and Sanford I. Weill Medical College of Cornell University, New York, New York 10021*

Received February 17, 2003; E-mail: chsope@lsu.edu

**Abstract:** The aim of this study was to develop new strategies for analyzing molecular signatures of disease states approaching real-time using single pair fluorescence resonance energy transfer (spFRET) to rapidly detect point mutations in unamplified genomic DNA. In addition, the detection process was required to discriminate between normal and mutant (minority) DNAs in heterogeneous populations. The discrimination was carried out using allele-specific primers, which flanked the point mutation in the target gene and were ligated using a thermostable ligase enzyme only when the genomic DNA carried this mutation. The allele-specific primers also carried complementary stem structures with end-labels (donor/acceptor fluorescent dyes, Cy5/Cy5.5, respectively), which formed a molecular beacon following ligation. We coupled ligase detection reaction (LDR) with spFRET to identify a single base mutation in codon 12 of a K-ras oncogene that has high diagnostic value for colorectal cancers. A simple diode laser-based fluorescence system capable of interrogating single fluorescent molecules undergoing FRET was used to detect photon bursts generated from the molecular beacon probes formed upon ligation. LDR-spFRET provided the necessary specificity and sensitivity to detect single-point mutations in as little as 600 copies of human genomic DNA directly without PCR at a level of 1 mutant per 1000 wild type sequences using 20 LDR thermal cycles. We also demonstrate the ability to rapidly discriminate single base differences in the K-ras gene in less than 5 min at a frequency of 1 mutant DNA per 10 normals using only a single LDR thermal cycle of genomic DNA (600 copies). Real-time LDR-spFRET detection of point mutations in the K-ras gene was accomplished in PMMA microfluidic devices using sheath flows.

### Introduction

Diseases such as cystic fibrosis, Alzheimer's, sickle cell anemia, and certain cancers are associated with changes in the sequence of particular genes. These changes can serve as biomarkers and may be useful for medical diagnosis at early stages of the disease. Since the majority of mutations in genetic disorders are due to variations such as point mutations, insertions, or deletions, it is required that diagnostic techniques being developed have the capability of distinguishing these changes in a mixed population, where in most cases the mutant allele is the minority. In addition, DNA diagnostic methods should be rapid, highly sensitive, cost-effective, and easy to perform.

Current approaches used to detect single nucleotide polymorphisms include homogeneous methods such as the template directed dye terminator incorporation (TDI) assay,<sup>1</sup> the 5'-nuclease allele specific hybridization TaqMan assay,<sup>2,3</sup> the allele specific molecular beacon assay,<sup>4</sup> and ligase detection reaction

(LDR).<sup>5-7</sup> These assays utilize fluorescence resonance energy transfer (FRET) to distinguish normal from mutant DNA without requiring a separation step, typically incorporated in most heterogeneous assays. In general, these FRET-based methods require preamplification of genomic DNA via PCR. However, PCR has some limitations that make it difficult to quantitatively analyze and detect genetic variations due to nonlinearities in amplicon number with cycle number. In addition, long optimization and set up times, long run and analyses times and the high level of inaccuracy and variation due to cross-contamination diminishes the probability of mutation screening assays incorporating PCR to perform measurements in real-time.

Recently, alternative methods have been developed to directly analyze genomic samples, which do not require PCR amplification. Lizardi and co-workers applied rolling circle amplification

(2) Holland, P. M.; Abramson, D. R.; Watson, R.; Gelfand, H. D. *Proc. Natl. Acad. Sci. U.S.A.* **1991**, *88*, 7276-7280.

(3) Livak, K. J.; Marmaro, J.; Todd, A. J. *Nat. Genet.* **1995**, *9b*, 341-342.

(4) Tyagi, S.; Bratu, D. P.; Kramer, F. R. *Nat. Biotechnol.* **1998**, *16*, 49-53.

(5) Barany, F. *Proc. Natl. Acad. Sci. U.S.A.* **1991**, *88*, 189-193.

(6) Chen, X.; Livak, K. J.; Kwok, Y. P. *Genome Res.* **1998**, *8*, 549-556.

(7) Landegren, U.; Kaiser, R.; Sanders, J.; Hood, L. *Science*, **1988**, *241*, 1077-1080.

<sup>†</sup> Louisiana State University.

<sup>‡</sup> Joan and Sanford I. Weill Medical College of Cornell University.

(1) Chen, X.; Kwok, Y. P. *Nucleic Acids Res.* **1997**, *25*, 347-353.

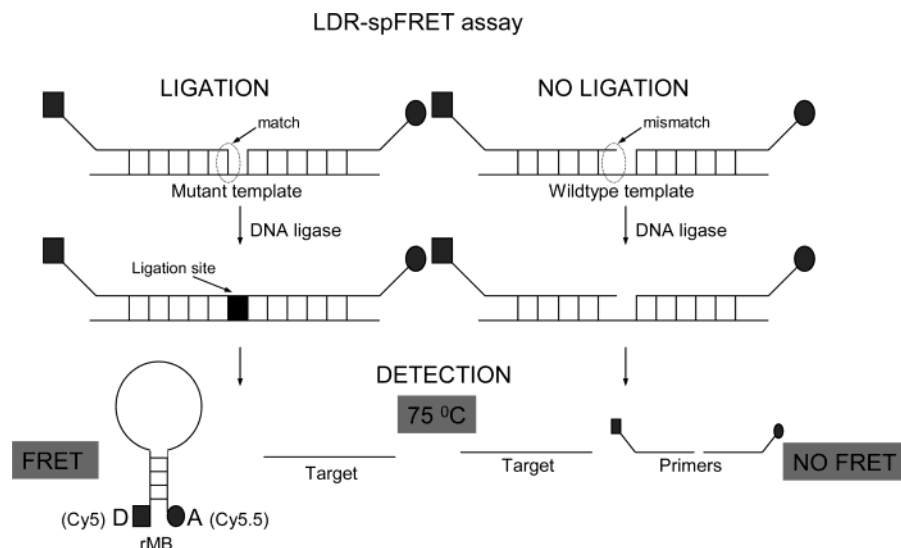


**Figure 1.** Illustration of the LDR–spFRET assay in which two allele-specific primers are labeled at their 3′- and 5′-ends with fluorescent dyes. These primers flank a single base mutation on the target template. Each primer has a complementary arm sequence. Thermal stable DNA ligase covalently joins the two adjacent primers when perfectly matched to the template, forming a molecular beacon that can undergo FRET. Conversely, the unligated primers do not show FRET. The detection temperature of the assay was maintained at 75 °C to melt the duplex formed between the target and LDR primers as well as stem sequences of unligated primers but not the stem of the fully formed beacon.

(RCA), a technique driven by DNA polymerase, to replicate circularizable probes with either linear or geometric hyperbranched kinetics under isothermal conditions.<sup>8,9</sup> In another report, Hall and co-workers used a serial invasive signal amplification reaction (SISAR), which generated  $10^7$  reporter molecules for each molecule of DNA in a 4 h reaction that could detect as few as 600 copies of a methylene tetrahydrofolate reductase gene in a sample of human genomic DNA.<sup>10</sup> While these methods avoid the use of PCR, the amplification times associated with these techniques typically exceed 60 min.

Another approach for detecting point mutations without PCR has been demonstrated using conductivity detection. Park and co-workers reported an array-based electrical detection method in which conductivity changes associated with the binding of an oligonucleotide labeled with gold nanoparticles to a target oligonucleotide.<sup>11</sup> This group applied the method for the detection of 500 fM target DNA with a point mutation selectivity factor of  $\sim 100\,000:1$ . Another electrochemical detection scheme for identification of single nucleotide alterations was demonstrated by Huang.<sup>12</sup>

Single-molecule photon burst detection offers a unique opportunity to monitor the presence of particular sequences directly in genomic DNA without the need for a PCR amplification step. In one such report, Castro and co-workers developed a method for the rapid, direct detection of specific nucleic acid sequences.<sup>13,14</sup> In their approach, two peptide nucleic acid (PNA) probes complementary to different sites on a target DNA were used to detect these sequences in unamplified genomic DNA.

The two fluorescently labeled PNA probes were hybridized to the sample and analyzed using a laser-based fluorescence system capable of detecting single fluorescent molecules at different wavelengths (Rhodamin-6G and Bodipy-TR channel) simultaneously in a flow cell. Coincident signals in both channels indicated the presence of a target molecule while noncoincident signals indicated the absence of the target.

In another report, specific DNA sequences in a homogeneous assay were analyzed using labeled hairpin-shaped oligonucleotide probes (Smart-Probes) in combination with single molecule detection.<sup>15</sup> The smart probes consisted of a fluorescent probe (oxazine dye JA242) attached at one end of the hairpin structure. Oxazine dye is efficiently quenched by guanosine residues at the other end of the arm sequence of the molecular beacon. An increase in the fluorescence intensity was detected in the presence of a matched target sequence due to the separation of the dye from the guanosine residues. In the absence of a complementary target sequence, no fluorescence emission was observed.

In this paper, we wish to report a rapid, potentially real-time mutation detection scheme capable of detecting low abundant point mutations directly from unamplified genomic DNA. The detection scheme is illustrated in Figure 1. A ligase-based point mutation detection assay that uses an allele-specific discriminating primer and a common primer, each having a 10 base pair (bp) complementary arm with fluorescent labels at their 5′- and 3′-ends, is used. A perfect match between the base at the 3′-end of the discriminating primer and the target allows the ligase to covalently join the two adjacent primers flanking the mutation site. A reverse molecular beacon (rMB) is formed by the complementary arm sequences of the ligated primers. After ligation and denaturation of the duplex formed between the target DNA and ligated product, the rMB is formed because the stem is designed to have a higher thermal stability compared to the target/LDR-product duplex, bringing the dye labels in close proximity. Fluorescence emission resulting from the single-

- (8) Lizardi, P. M.; Huang, X.; Zhu, Z.; Bray-Ward, P.; Thomas, D. C.; Ward, C. D. *Nat. Genet.* **1998**, *19*, 225–232.  
 (9) Zhong, X.; Lizardi, M. P.; Huang, X.; Bray-Ward, L. P.; Ward, C. D. *Proc. Natl. Acad. Sci. U.S.A.* **2001**, *98*, 3940–3945.  
 (10) Hall, J. G.; Eis, P. S.; Law, S. M.; Reynaldo, L. P.; Prudent, J. R.; Marshall, D. J.; Allawi, H. T.; Mast, A. L.; Dahlberg, J. E.; Kwiatkowski, R. W.; Arruda, M. D.; Neri, B. P.; Lyamichev, V. I. *Proc. Natl. Acad. Sci. U.S.A.* **2000**, *97*, 8272–8277.  
 (11) Park, S. J.; Taton, T. A.; Mirkin, C. A. *Science* **2002**, *295*, 1503–1506.  
 (12) Huang, J. T.; Mingshun, L.; Knight, D. L.; Grody, W. W.; Miller, F. J.; Ho, C. M. *Nucleic Acids Res.* **2002**, *30*, e55.  
 (13) Castro, A.; Williams, J. G. K. *Anal. Chem.* **1997**, *69*, 3915–3920.  
 (14) Castro, A.; Okinaka, R. T. *Analyst* **2000**, *125*, 9–11.

- (15) Knemeyer, J.; Marmé, N.; Sauer, M. *Anal. Chem.* **2000**, *72*, 3717–3724.

pair FRET process can be detected in real time using single molecule detection.

Real-time spFRET measurements were performed in a poly-(methyl methacrylate) (PMMA) microfluidic device to detect rMB's formed in an LDR assay where point mutations in K-ras codon 12 (high association with colorectal cancer) were detected in unamplified genomic DNA. Also, we demonstrate the assay's capability to rapidly detect single-point mutations in genomic samples at a sensitivity of 1:1000 without PCR amplification. Analysis times < 5 min were achieved using real-time LDR-spFRET detection in the microfluidic device with only a single thermal cycle for the LDR.

## Experimental Section

**Genomic DNA Extraction from Cell Lines.** Genomic DNA was extracted from cell lines of a known K-ras genotype (HT29, wildtype; LS180, G12D (mutant)).<sup>16</sup> The cell lines were grown in RPMI culture media with 10% fetal bovin serum. Harvested cells ( $\sim 1 \times 10^7$ ) were resuspended in DNA extraction buffer (10 mM Tris-HCl, pH 7.5, 150 mM NaCl, 2 mM EDTA, pH 8.0) containing 0.5% SDS and 200  $\mu$ g/mL proteinase K and incubated at 37 °C for 4 h. NaCl (37% v/v of 6 M) was added to the mixture, and then the samples were centrifuged. DNA was precipitated from the supernatant with 3 volumes of EtOH, washed with 70% EtOH and resuspended in TE buffer (10 mM Tris-HCl, pH 7.2, 2 mM EDTA, pH 8.0).

**PCR Amplification of Genomic DNA.** PCR amplifications were carried out in 50  $\mu$ L of 10 mM Tris-HCl buffer (pH 8.3) containing 10 mM KCl, 4.0 mM MgCl<sub>2</sub>, 250  $\mu$ M dNTPs, 1  $\mu$ M forward and reverse primers (50 pmol of each primer), and between 1 and 50 ng of genomic DNA extracted from the cell lines. The primers used were as follows: Ex.1.3 forward = 5' AAC CTT ATG TGT GAC ATG TTC TAA TAT AGT CAC 3'; Ex.1.4 reverse = 5' AAA ATG GTC AGA GAA ACC TTT ATC TGT ATC 3'; Ex.2.9 forward = 5' TCA GGA TTC CTA CAG GAA GCA AGT AGT 3'; and Ex.2.11 reverse = 5' ATA CAC AAA GAA AGC CCT CCC CA 3'. After a 2 min denaturation step, 1.5 units of Amplitaq DNA polymerase (Perkin-Elmer, Norwalk, CT) was added under hot-start conditions, and amplification was achieved by thermal cycling for 35–40 cycles at 95 °C for 30 s, 60 °C for 30 s, 72 °C for 1 min, and a final extension at 72 °C for 3 min. PCR products were stored at –20 °C until required for the LDR assays.

**Microfluidic Devices.** spFRET was performed in a microfluidic device fabricated using a photolithographic procedure described elsewhere.<sup>17</sup> Briefly, microstructures were fabricated using LIGA (German acronym for lithography, electroplating, and molding) processing. A thin layer of PMMA was glued onto a stainless steel metal plate and exposed to X-rays through an X-ray mask to form the desired patterns. The exposed PMMA resist was removed using GG developer (20% tetrahydro-1,4-oxazine, 5% 2-amino-ethanol-1, 60% 2-(2-butoxyethoxy) ethanol, and 15% deionized water) and GG rinse (80% 2-(2-butoxyethoxy) ethanol and 20% deionized water). After mechanically polishing the microstructures to the appropriate height, we electroplated nickel into the PMMA voids on the stainless steel from a Ni-sulfamate bath, and then it was mechanically planarized and lapped.

The mold insert fabricated as described previously was mounted along with a PMMA substrate into an embossing machine. The mold insert and substrate were heated above the PMMA's glass transition temperature,  $T_g$  (107 °C), and pressed together using a controlled force (several kilonewtons) for 4 min and gradually cooled to a temperature below its  $T_g$ . The mold insert and substrate were then demolded, leaving the desired features in the PMMA polymer. A thin film of PMMA was used as a cover plate for the fabricated channel. The device was

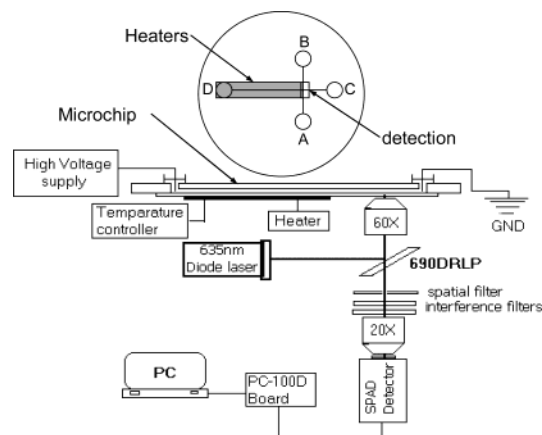


**Figure 2.** Near-IR single-molecule fluorescence detection system consisting of a diode laser ( $\lambda = 635$  nm) that was directed into a microscope objective using a dichroic and focused into the center of the fluidic channel approximately  $\sim 0.1$  mm from the cross junction. Fluorescence was collected by this same objective and imaged onto an aperture, through a set of FRET filters, and finally processed using a single-photon avalanche diode. Heaters were attached to the cover plate of the microfluidic device to regulate the temperature during detection and also to perform the LDR.

assembled by clamping a molded PMMA substrate and the cover plate between two glass plates and thermally annealing for 12 min at 107 °C and cooling to room temperature in a GC oven. Microdevices were fabricated in a “T” configuration and had channel sizes of 50  $\mu$ m wide and 100  $\mu$ m deep (see Figure 2 for device layout). Due to the low EOF and minimal analyte (DNA) adsorption associated with PMMA substrates, no modification was required on the wall of the PMMA devices used in our experiments.<sup>17</sup>

**Ligation Primers and rMB's.** The rMB models and LDR primers were synthesized by IDT (Integrated DNA technologies, Coralville, IA) using phosphoramidite chemistry on a commercial nucleic acid synthesizer (model ABI394) and RP-HPLC purified. Allele-specific ligation primers for identifying point mutations in codon 12 were designed based on the known sequence of the K-ras gene. A discriminating primer, 5'-Cy5-GCGGCGCAGCAAAACTGTGG-TAGTTGGAGCTGA-3' was designed to have a 10-bp stem sequence (underlined) that was end labeled with Cy5 (donor) at its 5'-end and a discriminating base at its 3'-end. A common primer, 5'-pTGGCGTAG-GCAAGAGTGCCCGCTGCGCCGC-Cy5.5-3' was fluorescently labeled with Cy5.5 (acceptor) at its 3'-end of a 10-bp arm sequence (underlined) and phosphorylated at its 5'-end. The arm sequences of the primers were complementary to each other but not to the target.

rMB models were designed and evaluated with the help of DNA folding software based on the work of the Zucker laboratory.<sup>18</sup> In the modeling studies, we adopted a strategy reported earlier by Zhang et al., where molecular beacons with two fluorophores instead of one and a quencher were used.<sup>19</sup> An rMB containing a 44-bp loop sequence flanked by a 10-bp arm sequence, 5'-Cy5-GCGGCGCAGCAAAACT-T G T G G T A G T T G G A G C T G A T G G C G T A G -GCAAGAGTGCCCGCTGCGCCGC-Cy5.5-3', was synthesized by IDT. The underlined sequence represents the complementary arms of the rMB. The length and the sequence of the rMB probe were chosen to match those of the two ligated primers specific for the point mutation in the K-ras gene. The  $T_m$  of the stem was designed to be higher than the  $T_m$  of the duplex formed between the hairpin loop and target DNA.

**Ligation Protocol.** LDR reactions were carried out in a 20  $\mu$ L reaction volume containing 0.25 units/ $\mu$ L thermostable DNA ligase (Ampligase, New England Biolabs), 20 mM Tris-HCl (pH 8.3), 25 mM KCl, 10 mM MgCl<sub>2</sub>, 0.5 mM NAD<sup>+</sup>, 0.01% Triton X-100, 10 pM of LDR primers, and a mixture of genomic DNA or PCR products at the

(16) Khanna, M.; Park, P.; Zirvi, M.; Cao, W.; Picon, A.; Day, J.; Paty, P.; Barany, F. *Oncogene*, **1999**, *18*, 27–38.

(17) Ford, S. M.; Davis, J.; Kar, S.; Qi, S. D.; McWhorter, S.; Soper, S. A.; Malek, C. K. *J. Biochem. Eng.* **1999**, *121*, 13–21.

(18) SantaLucia, J. *Proc. Natl. Acad. Sci. U.S.A.* **1998**, *95*, 1460–1465.

(19) Zhang, P.; Beck, T.; Tan, W. *Angew. Chem., Int. Ed.* **2001**, *40*, 402–405.

appropriate copy numbers. The DNA was denatured by heating the reaction mixtures to 94 °C prior to adding the ligase enzyme. Thermal cycling was performed in a Genetech thermocycler (Princeton, NJ) for 1–50 cycles using 1 min at 94 °C and 4 min at 65 °C. The reaction was stopped by cooling it rapidly to 4 °C and adding 0.5  $\mu$ L of 0.5 mM EDTA. For real-time analysis, LDR reagents were mixed with genomic DNA and loaded into a sample well of the microfluidic device. Thermal denaturation was performed at 94 °C using Kapton heaters attached directly to the microfluidic device followed by an annealing/ligation step at 65 °C for 4 min and subsequent on-chip single molecule detection.

**Instrumentation.** Single-pair FRET measurements were accomplished using an epi-illumination fluorescence system shown in Figure 2. The excitation source consisted of a diode laser (635 nm, 56DIB142/P1, Melles Griot, Boulder, CO). The laser was directed onto a focusing objective using a dichroic mirror (690DRLP, Omega Optical, Brattleboro, VT). The objective was a 60 $\times$ , 0.85 NA microscope objective that was used to focus the laser to a 5  $\mu$ m spot ( $1/e^2$ ) into the microchannel resulting in a detection volume of  $\sim$ 1.5 pL. The fluorescence was collected by this same objective and transmitted through a set of filters specific for Cy5.5. The dichroic mirror transmitted Cy5.5 fluorescence that was further isolated using a set of filters consisting of a 690 nm long-pass and band-pass filter (710DF10, Omega Optical, Inc, Brattleboro, VT). The light was then passed through a 100- $\mu$ m diameter aperture and focused onto the active area of an avalanche photodiode (SPCM-AQ-141, EG&G, Vandreuil, Canada) using a 20 $\times$  objective. Transistor–transistor logic (TTL) pulses from the photodiode were counted by a PC plug in board (PC100D, Advanced Research Instruments, Boulder, CO), stored, and subsequently analyzed by a Pentium PC computer.

**Electrokinetic Pumping.** LDR samples from the conventional thermocycler were diluted with ddH<sub>2</sub>O before loading into the microfluidic device. Dilution was carried out so as to minimize high currents generated during electrophoretic pumping due to the high salt concentration in the reaction buffer. Electrokinetic pumping was carried out by applying 375 V/cm along the channel marked C–D in Figure 2. The LDR sample was placed in reservoir D, and TBE buffer (pH 8.0), into reservoir C. For single-molecule experiments where rare events in heterogeneous populations were to be counted, sampling efficiency is a critical parameter that must be considered. Electrokinetic focusing has previously been used to improve sampling efficiency for SMD in microfluidic devices.<sup>20,21</sup> In our experiments, electrokinetic focusing was accomplished by applying voltages to reservoirs A and B on the microfluidic device so as to confine the samples (rMB's) within a narrow stream ( $\sim$ 15  $\mu$ m width) at a detection point located  $\sim$ 100  $\mu$ m from the tee junction. The focusing voltages were generated by applying  $-200$  V at both reservoirs. The resulting sampling efficiency was estimated to be  $\sim$ 33% compared to a sampling efficiency of only 10% for unfocused flow.

**Data Analysis.** Autocorrelation analysis has been shown to be an effective tool for demonstrating the presence of nonrandom correlated bursts of photons due to single molecules and characterizing transit times of these particles.<sup>22,23</sup> The autocorrelation function,  $A(\tau)$ , was calculated using the relationship

$$A(\tau) = \frac{1}{N} \sum_{t=0}^{N-1} d(t) d(t + \tau) \quad (1)$$

where  $N$  is the total number of points in the data stream,  $d(t)$  is the data point at time  $t$ , and  $d(t + \tau)$  is the data point at time  $t + \tau$  ( $\tau$  is the delay interval). In our experiments, the autocorrelation was com-

puted over the entire data set, which consisted of a 50 s total accumulation time with each data point representing 2 ms (total number of points = 25 000) unless otherwise stated. Individual molecules were examined using a weighted quadratic summing (WQS) filter given by<sup>22,23</sup>

$$S(t) = \sum_{\tau=0}^{k-1} \omega(\tau) d(t + \tau)^2 \quad (2)$$

where  $k$  is a range that covers a time interval equal to the molecular transit ( $k = 4$  corresponding to 8 ms in the present experiments). To best distinguish the single-molecule photon bursts from the random background noise, the weighing factor,  $\omega(\tau)$ , was chosen as an asymmetrical ramp,  $\omega(\tau) = (\tau + 1)/k$  for  $\tau = 0$  to  $k - 1$ ; otherwise  $\omega(\tau) = 0$ . The quadratic form in eq 2 produced a numerical output that could be readily processed by a threshold discriminator or peak detector to indicate the presence of a fluorescent molecule (event).

In most SMD applications, a molecular detection threshold is used to distinguish single-molecule fluorescence bursts from random fluctuations in the background. The optimum value for this threshold maximizes detection efficiency and, at the same time, minimizes false positives. The threshold value was determined by evaluating data from control samples (wild-type only DNA) and selected to produce average false positive rates of 0 s<sup>-1</sup>. Histograms of fluorescence burst distributions for the single rMB's were accumulated using output values from the WQS filtered data set. These histograms were constructed by increasing the threshold value in fixed increments and counting the number of peaks exceeding that particular threshold level. Peaks were counted only once in a typical analysis.

## Results and Discussion

**Ligase Detection Reaction.** LDR relies on a ligase chain reaction (LCR) that was first developed by Barany in 1991, where thermostable DNA ligase enzyme was used to discriminate between normal and mutant DNA and amplify the allele-specific product.<sup>5</sup> A mismatch at the 3'-end of the discriminating primer prevents the DNA ligase from joining the two fragments together. Using only one pair of primers in a reaction results in a linear amplification called the ligase detection reaction (LDR). The high fidelity of LDR to distinguish matched target in a large population of mismatches relies on the ability of the thermostable ligase enzyme to rapidly dissociate from the target containing a mismatch.<sup>24</sup> As a result, LDR has demonstrated a high level of specificity that is very suitable for mutation screening and detection of low abundant mutations.

**rMB Studies.** Molecular beacons are hairpin-shaped oligonucleotides with a stem formed by complementary bases. Conventional molecular beacon's loop fragment is designed to hybridize with a target resulting in a thermodynamically more stable hybrid with the target molecule compared to the stem hybrid.<sup>25</sup> Because the stem configuration is disrupted, quenching of the fluorescent probe is disrupted and donor fluorescence appears. In our approach, rMB's were designed in that the thermal stability of the stem was greater than that of the duplex formed between the target and loop. This was achieved by adopting suitable conditions of concentration, ionic strength, temperature, and stem sequence with high GC content.<sup>25,26</sup> The melting temperatures of the stems were predicted using a DNA folding program (Zucker folding program, [\(20\) Haab, B. B.; Mathies, R. A. \*Anal. Chem.\* \*\*1999\*\*, \*71\*, 5137–5145.](http://www.bioin-</a></p>
</div>
<div data-bbox=)

(21) Jacobson, C. S.; Ramsey, J. M. *Anal. Chem.* **1997**, *69*, 3212–3217.

(22) Shera, E. B.; Seitzinger, N. K.; Davis, L. M.; Keller, R. A.; Soper, S. A. *Chem. Phys. Lett.* **1990**, *174*, 553–557.

(23) Soper, S. A.; Mattingly, Q.; Vegunta, P. *Anal. Chem.* **1993**, *65*, 740–748.

(24) Khanna, M.; Cao, W.; Zirvi, M.; Paty, P.; Barany, F. *Clin. Biochem.* **1999**, *32*, 287–290.

(25) Tyagi, S.; Kramer, F. R. *Nat. Biotechnol.* **1996**, *14*, 303–308.

(26) Orbons, L. P.; van der Marel, G. A.; van Boom, J. H.; Altona, C. *Nucleic Acids Res.* **1986**, *14*, 4187–4196.

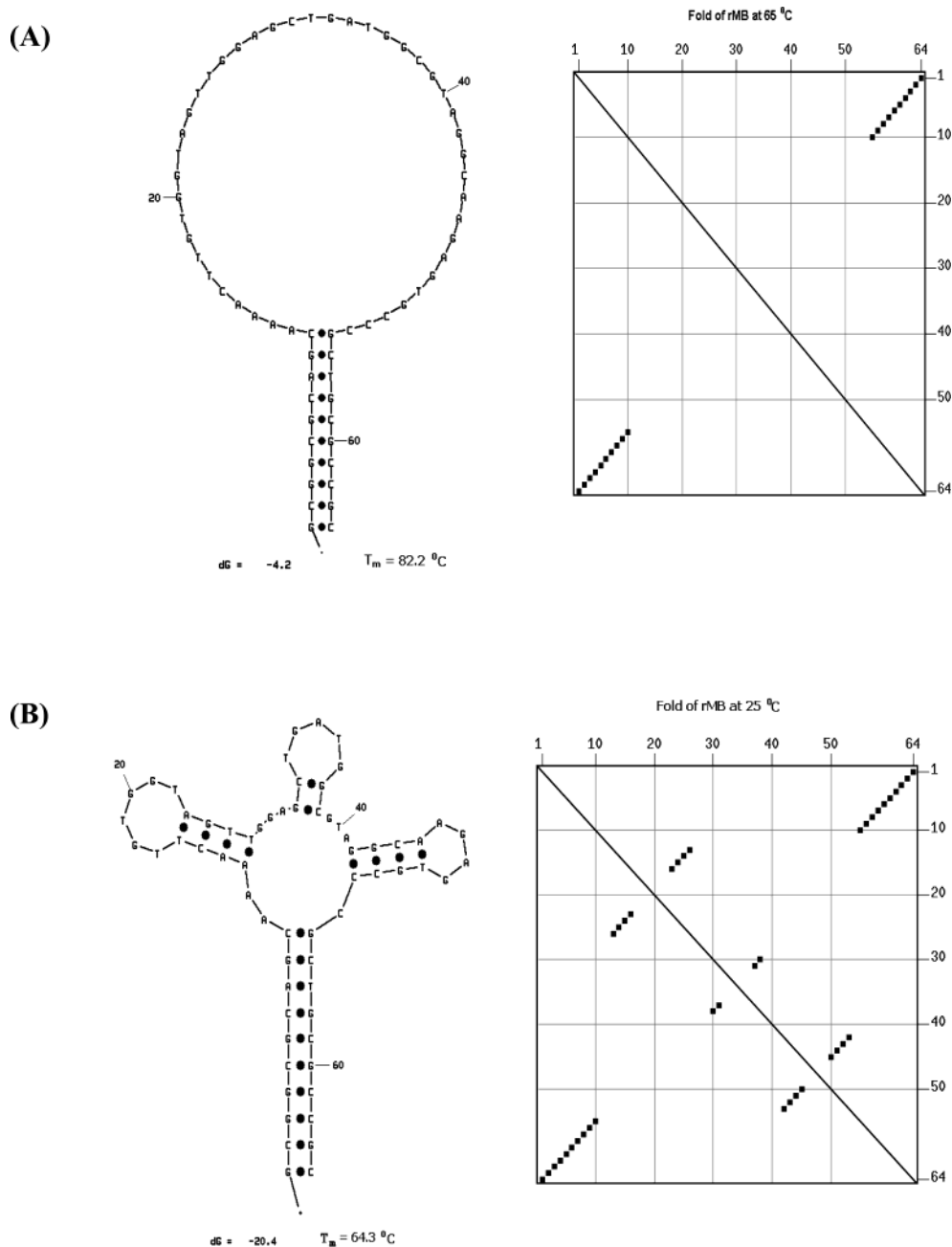


**Figure 3.** Computed secondary structure and energy dot plot generated from a 64-bp oligonucleotide consisting of a complementary stem sequence (10 bp) and loop sequence (44 bp). The folding temperature was performed at 65 °C (A) or 25 °C (B) using the Zuker DNA folding program. The dots (■) on the energy dot plot represent optimal folding within the structure.

fo.rpi.edu/applications/mfold/old/dna/form1.cgi) which utilizes the free energy of formation of the stem to predict the melting temperature ( $T_m$ ).

Figure 3A shows computed secondary structures of a 64-bp MB (see Experimental Section for sequence) folded at 65 °C, 25 mM NaCl, and 10 mM MgCl. The  $T_m$  of the 10-bp stem was determined to be 82.2 °C. The dot plots on the right of each structure shows optimal folding that resulted from base pairing between the  $i$ th and  $j$ th base (a dot in row  $i$  and column  $j$  represents a base pair). The dots represent the superposition of all possible suboptimal folding that may occur within  $p\%$  of the minimum free energy, where  $p$  is the maximum percent deviation from the minimum free energy. At a folding temperature of 65 °C (see Figure 3A), only one structure is obtained. When the folding temperature was lowered to room temperature,

the same MB sequence generated multiple structures including the one shown in Figure 3B with a stem melting temperature of 64.3 °C. At lower temperatures, nonspecific binding may occur within the probe sequence forming alternate structures with multiple loops or dimeric complexes. The alternate conformations result in subpopulations with potentially lower energy transfer efficiencies between the two fluorescent probes. In this assay, the detection temperature was set to be > 65 °C so that nonspecific binding resulting in FRET-diminishing configurations were minimized and, as a result, only one stable rMB structure shown in Figure 3A was the predominant form.

The design of our rMB was also based on earlier studies where thermodynamic behaviors of partially self-complementary DNA molecules were studied.<sup>27,28</sup> According to these studies, it was observed that, in aqueous solution at low concentrations,

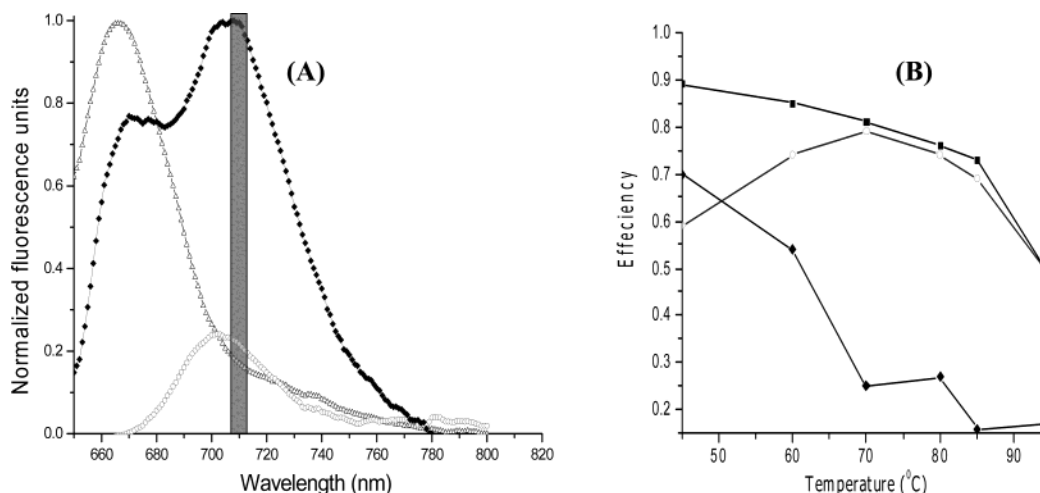


**Figure 4.** (A) Emission spectra of Cy5 ( $\Delta$ ), Cy5.5 ( $\circ$ ) labeled primers, and the rMB ( $\blacklozenge$ ) labeled with both fluorophores in Tris-HCl buffer, pH 7.6, at 70 °C. The concentration of the primers and the rMB was set to 200 nM. The pass band of the filter is shown, which was used for the single-molecule detection (shaded box). (B) Temperature studies showing an energy transfer efficiency ( $E$ ) of 200 nM of the 64-bp rMB in the presence ( $\circ$ ) and absence ( $\blacksquare$ ) of a 44-bp template (complementary to the loop sequence) and 7 M urea ( $\blacklozenge$ ) in 2 $\times$  SSPE buffer, pH 7.5. The energy transfer efficiency between Cy5 and Cy5.5 were determined using eq 3, where rMB's labeled with only one dye at the 5'-end was used to determine  $F_a$ . The samples were excited at 625 nm.

oligonucleotide molecules having a probe sequence flanked by two complementary arms may exist in equilibrium between two structured conformations; the dimeric duplex or monomeric hairpin. When the temperature was increased, the equilibrium shifted toward the hairpin conformation. In addition, these authors showed that the melting of hairpins is a monomolecular process, since it is independent of concentration, while duplex melting was a bimolecular process that was concentration dependent. Generally, single-molecule experiments require the probability of occupancy within the detection volume of a single molecule be significantly smaller than unity to lower the probability of double occupancy. This can be achieved using samples of low concentrations, and as such, the stability of the hairpin conformation over the duplex would be favored. Moreover, denaturation enthalpy changes for hairpins, and duplexes have shown that the presence of the loop stabilizes the hairpin with respect to the stem “only” duplex.<sup>27</sup> This phenomenon is attributed to stacking between the bases in the loop and the stem. Because the working concentrations of LDR primers and genomic DNA were low, it was expected that the  $T_m$  of the duplex formed from the single primer species in the LDR assay would be low and could be disrupted by increasing the detection temperature. This would lower or eliminate the background arising from nonspecific hybridization of the primer stems. Analysis of the duplex formed between the stems of unligated LDR primers indicated a  $T_m$  of 47.3 °C at 250 nM, while the  $T_m$  of the stem duplex formed from the molecular beacon was 82.2 °C.

FRET depends on the inverse sixth power of the distance between the two probes ( $r^{-6}$ ), with the efficiency ( $E$ ) of energy transfer expressed as

$$E = \frac{R_0^6}{R_0^6 + r^6} = 1 - \left( \frac{F_{da}}{F_d} \right) \quad (3)$$

where  $F_{da}$  is the fluorescence intensity of donor in the presence

of acceptor,  $F_d$  is the intensity in the absence of acceptor,  $r$  is the distance between the donor and the acceptor, and  $R_0$  is the Förster radius. Due to the large spectral overlap ( $\sim 86\%$ ) between Cy5 and Cy5.5 producing an exceptionally high  $R_0$  value (63.3 Å), flexibility in the choice of linker structures attaching the dyes to the rMB could be used.

The emission spectra of singly labeled Cy5 and Cy5.5 primers and an rMB having 10-bp arms end labeled with both dyes are shown in Figure 4A. As can be seen, excitation at 625 nm does produce some emission from Cy5.5. Direct excitation from Cy5.5 may produce false positives in the assay, since this signal would not depend on a successful ligation. However, single-molecule detection experiments performed directly on singly labeled Cy5 and Cy5.5 primers indicated no detectable single-molecule events above a preselected threshold level after the data was subjected to the WQS filter.

To determine the stability of the rMB, thermal and chemical studies were carried out in a 2 $\times$  SSPE buffer (pH 7.5). The transfer efficiency ( $E$ , see eq 3) for the rMB model as a function of temperature is shown in Figure 4B. At low temperature, FRET transfer efficiency of the rMB in the presence of a complementary template was lower than those of rMB's in its absence. Low  $E$  values at lower temperatures were due to effective competition between hybrids formed between the stem of the rMB and the duplexed DNA. However, increasing the temperature favors the hairpin with a concomitant increase in  $E$  ( $\sim 0.8$ ) due to its increased thermodynamic stability. At higher temperatures,  $E$  drops again due to further transition from the hairpin structure to a random coil (thermal denaturation of the stem). The melting temperature of the stem in the rMB was determined experimentally to be  $\sim 80$  °C, which was comparable to the theoretical value of 82.2( $\pm 4.0$ ) °C obtained using the DNA folding program.<sup>18</sup>

**Single-Pair FRET Detection.** LDR primers were designed to detect point mutations in codon 12 of the K-ras gene associated with colorectal cancer.<sup>29,30</sup> For this particular muta-

(27) Xodo, L. E.; Manzini, G.; Quadrioglio, F.; van der Marel, G. A.; van Boom, J. H. *Nucleic Acids Res.* **1986**, *14*, 5389–5398.

(28) Senior, M. M.; Jones, R. A.; Breslauer, K. J. *Proc. Natl. Acad. Sci. U.S.A.* **1988**, *85*, 6242–6246.

(29) Zhu, D.; Keohavong, P.; Finkelstein, S. D.; Swalsky, P.; Bakker, A.; Weissfeld, J.; Srivastava, S.; Whiteside, T. L. *Cancer Res.* **1997**, *57*, 2485–2492.

(30) Bos, J. L. *Mutat. Res.* **1988**, *195*, 255–271.

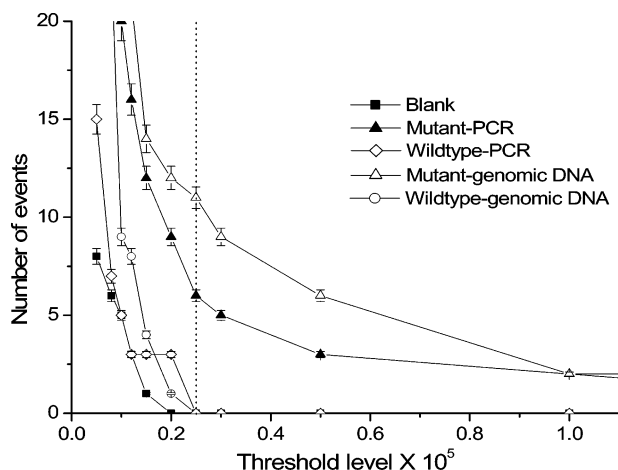


**Figure 5.** Plots showing the number of events detected versus threshold level for a 20 cycle LDR having  $\sim 3000$  copies of template and 10 pM primer concentrations. The templates used were diluted from PCR products or genomic DNA samples extracted from cell lines of known K-ras genotype. The dotted line indicates the threshold level,  $S(t) = 25\,000$ , which was chosen to set the false error detection probability to zero.

tion, the second position in codon 12, GGT, coding for glycine, mutates to GAT coding for aspartate, which can be detected by ligation of an allele-specific primer having a discriminating base and a phosphorylated common primer.

Typically, LDR assays are coupled to a primary PCR reaction with the amplicons used as templates for the ligation reaction.<sup>16,24,31</sup> To evaluate the efficiency of LDR directly on genomic DNA, we carried out spFRET studies using PCR products and genomic DNA extracted from cell lines containing known K-ras genotypes. Figure 5 shows plots of the number of single rMB's detected at various threshold levels for an LDR assay having  $\sim 3000$  copies (10 ng) of initial wildtype and mutant templates for both PCR product and genomic samples. A blank having no template was also analyzed. Applying 20 LDR cycles and assuming 100% ligation efficiency for each cycle, one would expect  $\sim 60\,000$  LDR products. LDR samples were diluted with water to a concentration where the probability of occupancy ( $P_o$ ) of a single rMB was  $\sim 2.2 \times 10^{-3}$ , which was calculated from<sup>32</sup>

$$P_o = CN_A P_v \quad (4)$$

where  $C$  is the analyte concentration,  $N_A$  is the Avogadro's number, and  $P_v$  is the probe volume (1.5 pL). The number of rMB's passing through the probe volume per unit time ( $N_{ev}$ ) was calculated from<sup>23</sup>

$$N_{ev} = \frac{2P_o v_{ep}}{\pi \omega_o} \quad (5)$$

where  $v_{ep}$  is the migration velocity of DNA (determined from the autocorrelation analysis of the data stream) and  $\omega_o$  is the  $1/e^2$  beam waist (5  $\mu\text{m}$ ). Therefore, with a concentration of  $\sim 30\,000$  copies in the 20- $\mu\text{L}$  sample well, we would expect  $\sim 28$  events per 100 s. From Figure 5, we did not detect any events above threshold (see dotted line in Figure 5) for either the wildtype PCR products or genomic DNA during the 100 s

acquisition time. Conversely, we did observe events from LDR products formed by mutant samples having a T/A match. Found above a threshold level from PCR product and genomic DNA samples were 6 and 12 events, respectively. These results indicate that LDR can be performed directly on genomic DNA. Based on these numbers, a detection efficiency of 42% was calculated. Our calculated detection efficiency should be considered provisional, since the number of events expected depends on the ligation efficiency for each thermal cycle, which was assumed to be 100%.

However, the average efficiency of ligation could be potentially enhanced by optimizing the LDR conditions. This can be achieved by altering the buffer conditions (salts, polyamines), enzyme concentration, or thermal-cycling times and temperatures.<sup>5</sup>

Studies were next performed on genomic samples containing a minority of mutant templates in a majority of wildtype to determine the ability of detecting low abundant point mutations using spFRET. Figure 6A shows fluorescence bursts from LDR samples having 600 copies (2 ng) of a mutant template in all reactions and changing the wild-type concentration with the ratio of mutant to wild-type varied from 1:1 to 1:1000. Clearly, the histogram in Figure 6B shows that single molecule events were observed from samples having the point mutation even at 1000 normal templates to 1 mutant.

The ligation efficiency of our LDR assay having different ratios of mutant:wild-type sequences was next investigated using digital spFRET detection. The wild-type copy number was varied from 600 to 600,000 while keeping the mutant copy number constant (600), resulting in a mutant:wild-type ratio of 1:1 to 1:1000. The average number of events (three replicates) from LDR rMB's detected above threshold in Figure 6 was plotted against the mutant to wild-type ratio as shown in Figure 7.

From this result, we note that the addition of wild-type sequences resulted in reduction of the formation of rMB's by the ligation reaction, suggesting that the wild-type template acts as a competitive inhibitor in the assay.<sup>24</sup>

In our previous examples using spFRET, we eliminated the sample processing overhead associated with PCR and performed the allele-specific LDR directly on genomic DNA. However, the assay still used linear amplification during LDR with a processing time of 100 min (20 cycles). Therefore, we attempted to perform spFRET using only a single LDR thermal cycle to significantly reduce the processing time without sacrificing information content from spFRET. Figure 8A shows fluorescence photon bursts resulting from LDR-produced rMB's linearly amplified using a ratio of 1 mutant to 10 wild-type sequences in the reaction cocktail. Five  $\pm 3.6$  events were detected using only one cycle for LDR. The histogram indicated no single-molecule events observed above threshold for 0 cycles. Similarly, the control sample having only wild-type sequences showed no bursts above threshold. A plot of the number of events versus cycle number is shown in Figure 8B. The plot was linear with a correlation coefficient of 0.989. The linear plot is consistent with the linear amplification process associated with LDR.

For the data secured previously using only a single LDR thermal cycle, the LDR reaction was performed directly in the PMMA microchip. The LDR reagents, mutant and wildtype genomic DNA (1:10 copy number ratio), were loaded into the

(31) Neiderhauser, C.; Kaempf, L.; Heinzer, I. *Eur. J. Clin. Microbiol. Infect. Dis.* **2000**, *19*, 477–480.

(32) Soper, S. A.; Legendre, B. L. *Appl. Spectrosc.* **1998**, *52*, 1–5.



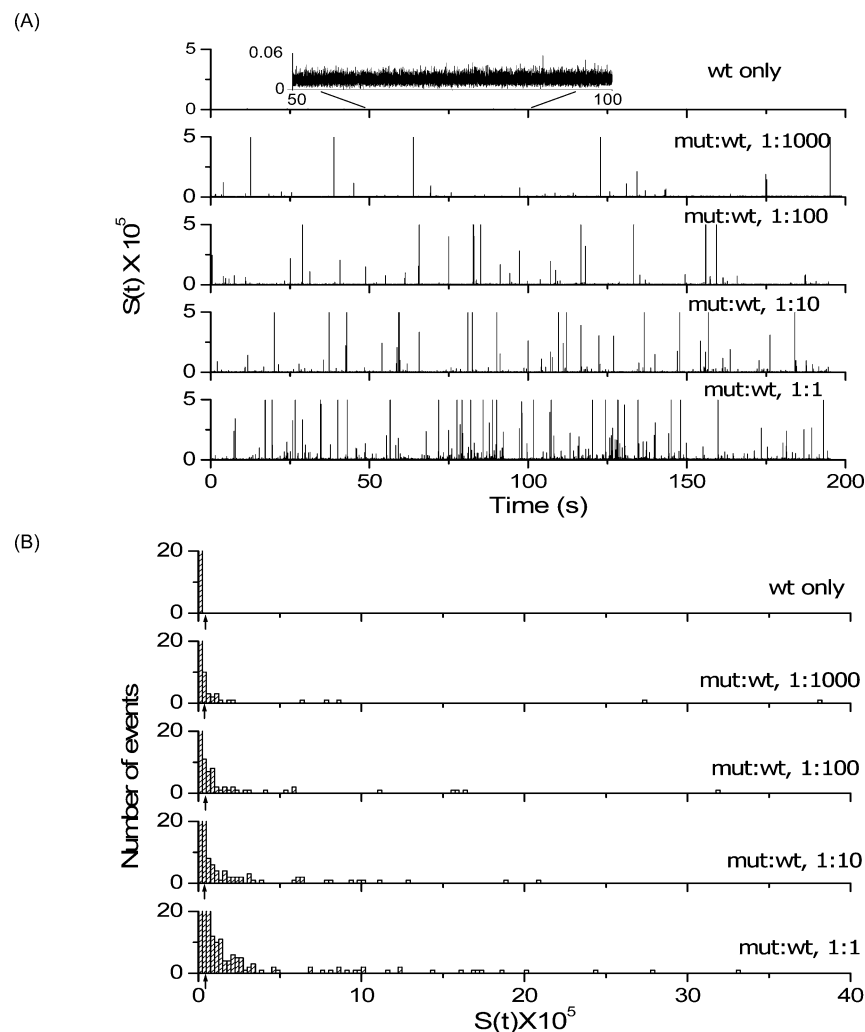


**Figure 6.** (A) Fluorescence bursts from individual rMB's formed as a result of a successful ligation reaction undergoing spFRET and (B) histograms showing the fluorescence photon burst distributions with the threshold value ( $S(t) = 25\,000$ ) indicated by an arrow. Genomic samples with ratios of mut:wt ranging from 1:1 to 1:1000 were used in the measurements. The initial mass of the mutant template in each assay was 2 ng.

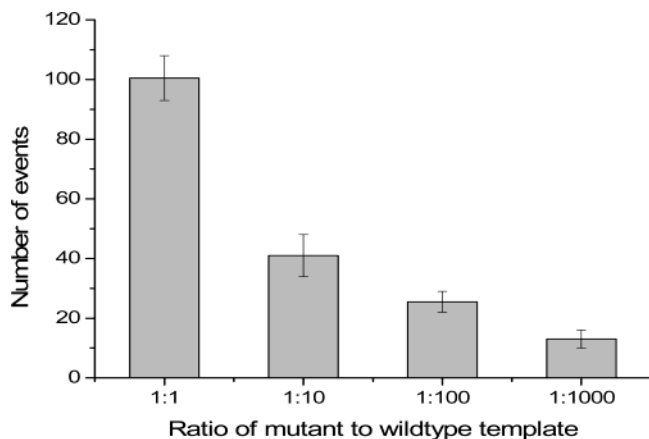


**Figure 7.** Histogram showing the average number (three replicates) of events detected from LDR-formed rMB's for different ratios of mut:wt with the copy number for the mutant remaining constant (600 copies).

sample reservoir of the microchip (see Figure 2) and allowed to migrate through the reaction channel (electrically driven) where the surface heating elements were situated to allow denaturation and subsequent ligation (5 min reaction time). This was followed by single-molecule detection at the desired temperature. As can be seen from the data displayed in Figure

8B, the number of events detected followed those expected based on the LDR cycle number. These data clearly show that mutation screening of mutant DNA in the presence of wild-type sequences using LDR and spFRET can be accomplished in under 5 min, providing near real-time molecular diagnostic information.

### Conclusions

The exquisite sensitivity of single-molecule detection can be used to eliminate processing steps required in multistep assays, reducing analysis time. In the present example, we eliminated the need for PCR amplification and performed an allele-specific ligation assay directly on genomic DNA. In addition, the high sensitivity afforded by single-molecule measurements also eliminated the need for thermal cycling during the ligation step. The specificity of the ligase enzyme toward mismatches coupled to spFRET of rMB's formed as a result of a successful ligation reaction for mutated DNA even in the presence of wild-type sequences provided near real-time molecular diagnostic screening even when the copy number of mutant sequences was low (600 copies).

Typical point mutation assays may require as much as 6–8 h to complete with most of the time overhead associated with generating enough material for readout via different amplifica-

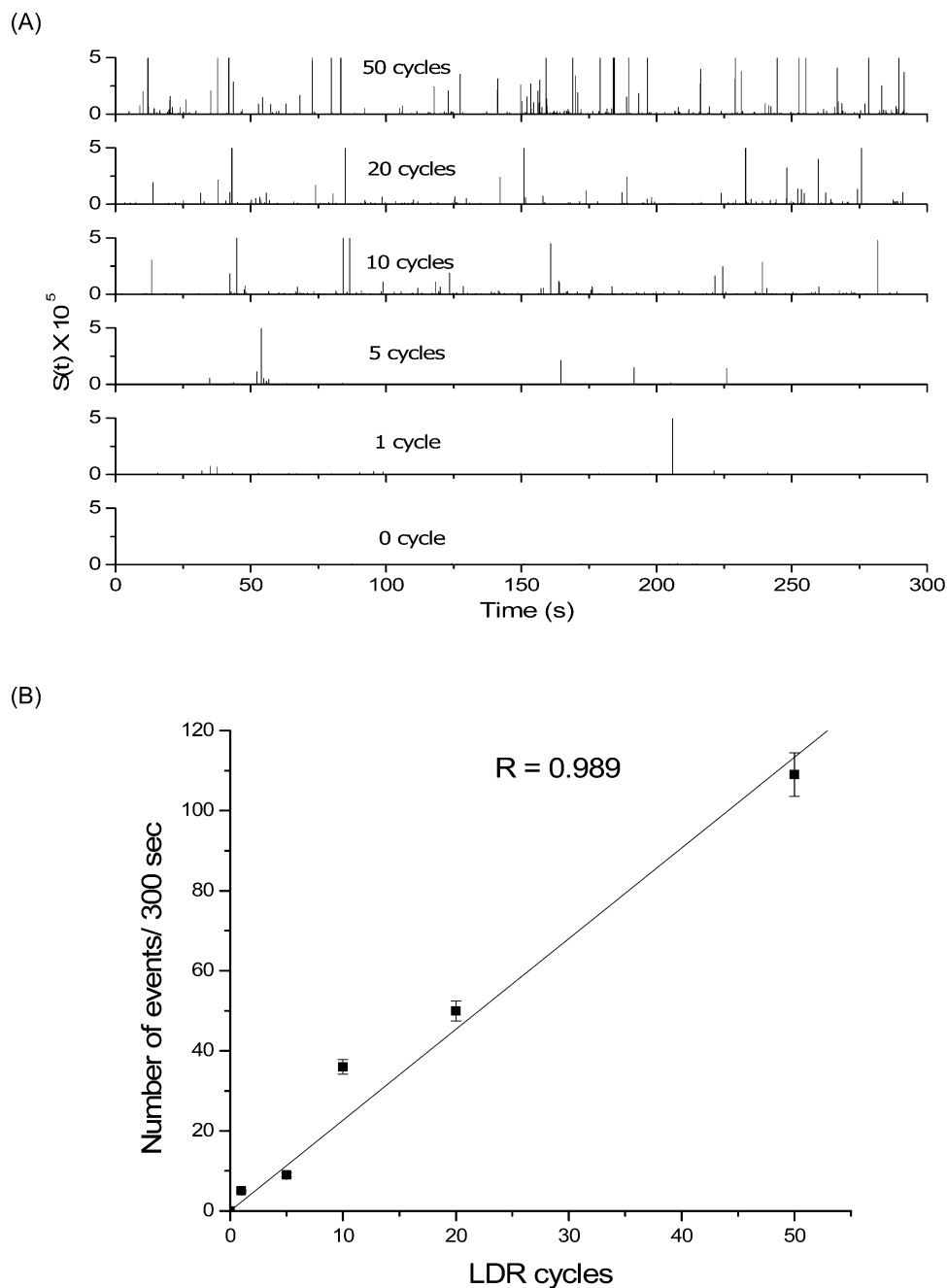


**Figure 8.** (A) Fluorescence bursts from individual rMB's undergoing spFRET as a function of the LDR cycle number. Genomic samples with a 1:10 ratio of mut:wt were used in the assay. The initial mass of the mutant template in each assay was 2 ng. (B) Linear calibration plot showing the number of LDR cycles versus number of fluorescence events.

tion strategies. Here, we have demonstrated the ability to do point mutation assays with a processing time of only 5 min, nearly 100 times faster than conventional methods. While much progress is being invested into reducing the processing time associated with PCR, the ability to perform mutational analysis directly on genomic DNA using single-molecule detection possesses other unique advantages, such as better quantification using digital molecular counting, reduced reagent requirements, and elimination of post-PCR purification/isolation steps. This assay format may find important applications in situations where

rapid high-volume identifications of genomic material (unique genomes or single nucleotide variations) are required.

**Acknowledgment.** The authors would like to thank the National Institutes of Health (R24-CA84625) for financial support of this work and the Center for Advanced Microstructures and Devices (CAMD) for their assistance in the fabrication of the molding dies used for embossing the microfluidic devices.

JA034716G